Non-linear registration of serial histological images of the middle ear

Shruti Nambiar[1], M. Mallar Chakravarty[2] and W. Robert J. Funnell[1,3]
[1]Department of BioMedical Engineering, McGill University, Montréal, Canada
[2]Pathophysiology and Experimental Tomography Centre, Aarhus University Hospital, Aarhus, Denmark
[3]Department of Otolaryngology, McGill University, Montréal, Canada

1. INTRODUCTION

Hearing loss is a relatively common disorder. Detailed analyses of the mechanical and acoustical properties of the middle ear have significant clinical implications. The finite-element method is a powerful tool, often used for such analysis. A comprehensive and reliable 3-D finite-element model of the human middle ear can provide a better understanding of the biomechanics of its many interrelated structures.

The middle ear extends from the eardrum (tympanic membrane) to the oval window (the interface with the inner ear) as shown in Fig. 1. The air-filled cavity contains three bones (malleus, incus and stapes), two muscles (tensor tympani and stapedius) and several ligaments and other structures. The 3-D geometries of finite-element models of the middle ear are often based on microscopic X-ray computed tomography (microCT) or magnetic resonance microscopy (MRM). Currently, these imaging modalities have limited resolution in comparison with the size of the middle-ear so it is not possible to distinguish details like the different tissue types in the ear canal, the fine details of the middle-ear ligaments and joints, and the distinct calcified and uncalcified components of the joint cartilage. Histological images offer much better image contrast and resolution. For example, the histological image of a middle-ear joint shown in Fig. 2 clearly shows details such as the joint capsule and the presence of synovial fluid within the joint. Such details are visible only in histological images and are important for realistic modelling of middle-ear mechanics and acoustics.

Serial histological sections have sometimes been used as the basis of 3-D finite-element models (e.g., Funnell et al., 1992; Warrick and Funnell, 1998; Sun et al., 2002) but serious spatial misalignments are introduced at the time of histological tissue processing. Registration algorithms are often employed to correct these distortions. Linear transformations have been used in the past to register, or align, middle-ear images with one another, but this cannot correct for all of the distortions. Non-linear registration techniques also exist and one such algorithm has been used for serial histological images of the brain (Chakravarty et al., 2006). The application of that non-linear warping algorithm to human middle-ear histological data was introduced in a previous paper (Nambiar et al., 2007). In this paper, we discuss tuning of the algorithm for application to the middle ear and present further results.

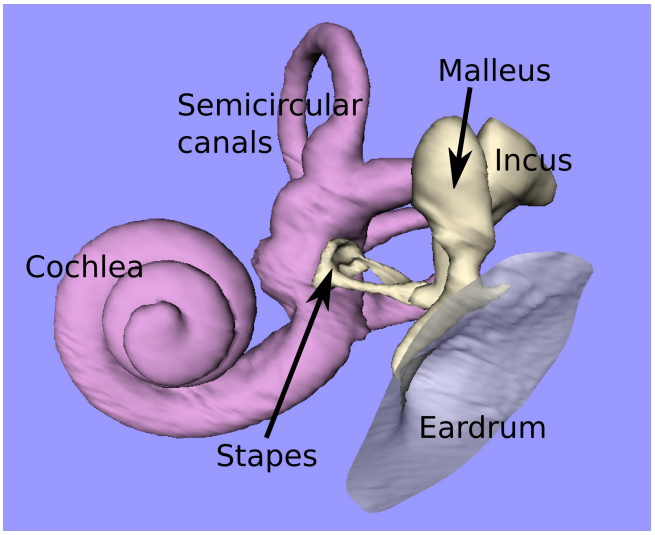

Fig. 1: Anatomy of the human ear (anterior view).

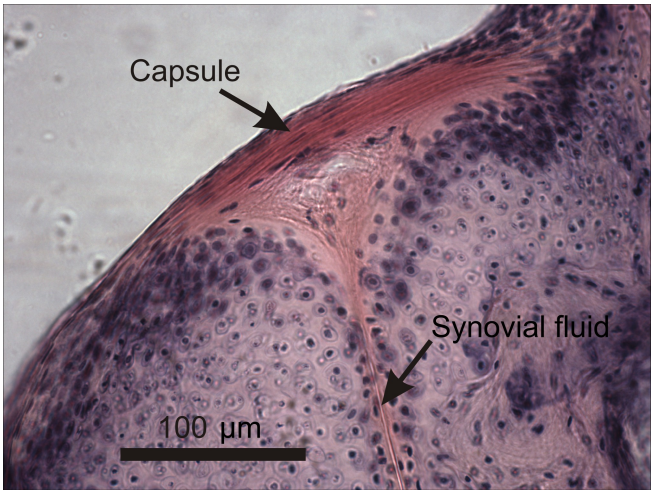

Fig. 2: Histological section of a middle-ear joint.

2. MATERIALS AND METHODS

2.1 Histological data acquisition

The histological data set for an adult human middle ear was acquired from C. Northrop (Temporal Bone Foundation, Boston). The histological block was cut into 20-µm-thick sections and every tenth slice was stained with hæmatoxylin and eosin to yield a total of 56 slices. Each slice was digitized using a slide scanner to form images of size 3644×2152 pixels. The images were then downsampled by a factor of 4 for improved processing speed.

2.2 Segmentation

The contours of the structures of interest were semi-automatically identified using Fie, a locally developed programme (http://audilab.bmed.mcgill.ca/~funnell/AudiLab/sw/fie.html).

2.3 Non-linear registration algorithm

The non-linear algorithm employed here is a variant of the Automatic Nonlinear Image Matching and Anatomical Labelling (ANIMAL) algorithm (Collins and Evans, 1997). The algorithm tries to maximize the slice-to-slice (source-to-target) anatomical consistency between adjacent slices in order to achieve global 3-D consistency. The ANIMAL algorithm defines a 2-D regular lattice of control nodes and computes a deformation vector for each node that maximizes the correlation ratio for the local intensity neighbourhood centred at each of these nodes. The non-linear spatial registration transformation is computed in a hierarchical fashion: deformations are first estimated on slices blurred with a Gaussian kernel having a large full width at half maximum (FWHM) and then the transformations are further refined by estimating deformations on slices blurred with Gaussian kernels having smaller FWHM's. This blurring is done three times. For each FWHM the ANIMAL algorithm calculates the deformation vector iteratively, with each iteration consisting of two steps: the first step involves calculation of a local translation for each node and the second is a smoothing step that ensures the continuity of the deformation fields and accounts for any stretching, tearing or overlap of the data. The non-linear transformations are represented by these deformation fields, which are defined to be locally translational. The overall optimization is thus achieved by amalgamation of all the local optimizations computed at each lattice point.

The non-linear transformation can be controlled by three parameters: the *similarity cost ratio*, the *stiffness* and the *weight*. These parameters play an important role in the transformation estimation at each level of blurring of the source and target images. The *similarity cost ratio* balances the similarity measure and the cost function. It is constant for all nodes defined by the ANIMAL algorithm at each resolution step. The *stiffness* parameter directly affects the nature of the deformation field calculated at each node. Large values for the stiffness parameter yield smooth deformation fields but may over-smooth local translations. Smaller stiffness values permit local translations but the estimated deformation could be discontinuous, which may cause tearing or overlapping of the image. The non-linear transformation is computed over a fixed number of iterations for each resolution step, and in each of these iterations a fraction of the local translation estimate is added to the current iteration according to the value of the *weight* parameter.

The three parameters were initially optimized by Chakravarty et al. (2006) for certain areas of the human brain (basal ganglia and thalamus). An exhaustive-search strategy was employed to minimize the mean chamfer distance between the transformed source contour data and the target contour data. In this study, the values of these optimization parameters were altered in a trial and error fashion such that the warping quality was enhanced over a set of sample slices.

The image-driven transformation thus obtained can be applied to the coördinates of the segmented contours, the surface triangulation of which yields a 3-D finite-element model.

3. RESULTS

Here we present preliminary results obtained by the application of the above algorithm. The final values of the optimization parameters described in Section 2.3 are shown in Table 1. In our study, the values of the parameters for the first two steps of blurring are equal to those estimated by Chakravarty et al.(2006). For the final step, a finer resolution (Gaussian kernel FWHM = 4 pixels) was used along with an increase in the stiffness and weight values.

Table 1: Parameters used for each of the resolutions

FWHM (in pixels)	Lattice diameter (in pixels)	Similarity	Stiffness	Weight
50	150	0.95	0.6	1.3
25	75	0.9	0.6	1.3
4	20	0.9	1	1

Sample histological images are shown in the figures to illustrate the registration principle. Fig. 3 shows the source slice, which is registered onto the

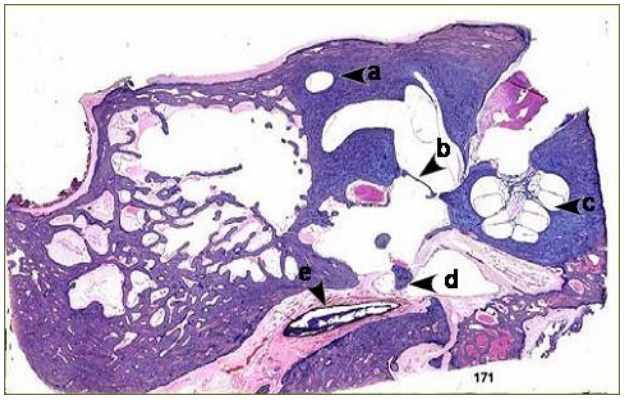

Fig 3: Source slice of human temporal bone.

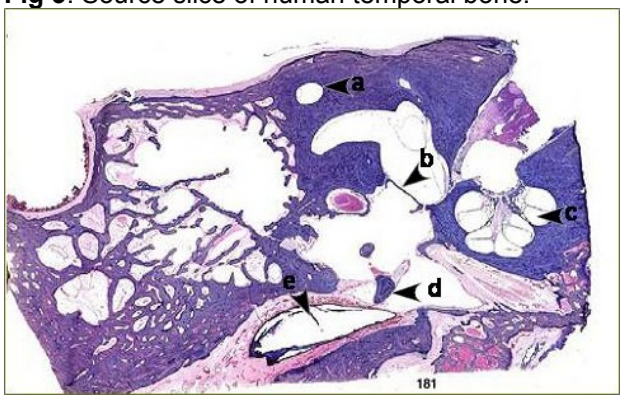

Fig 4: Target slice of human temporal bone.

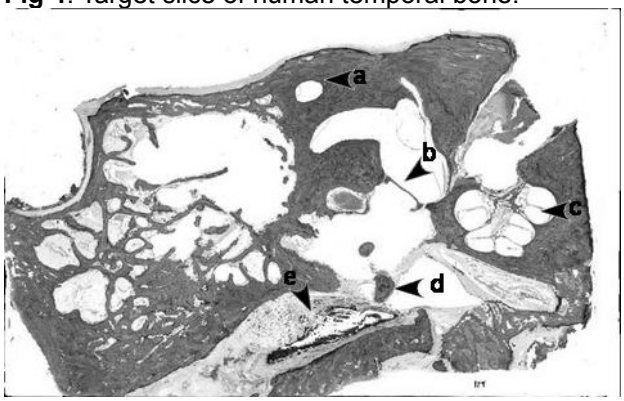

Fig 5: Source slice after registration.

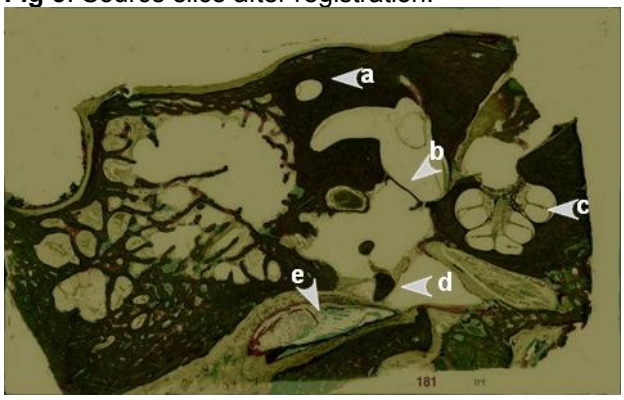

Fig 6:Registered source slice (in green) superimposed onto target slice (in red).

target slice (Fig. 4). Fig. 5 shows the source slice after registration. Some of the anatomical parts of the temporal bone are marked in the figures: (a) semicircular canal, (b) stapes footplate, (c) cochlea, (d) malleus, and (e) external ear canal. Fig. 6 shows the source slice, after registration, superimposed on the target slice. The geometries of the middle-ear substructures that are indicated by markers 'a', 'b', 'c' and 'd' are seen to have been successfully registered onto the target. However, the external ear canal (marker 'e') is badly distorted after registration. This is because the shape of the canal in the target slice is very different from that in the source slice. Certain artefacts in the areas indicated by markers 'a' and 'c' were clearly visible in the registered slice when values different from those given in Table 1 were used.

4. CONCLUSION

The results obtained from preliminary application of the registration algorithm indicate that good-quality alignments can be obtained for the structures of interest. Our future work will include a quantitative approach to choosing the optimization parameters that control the quality of the 2-D slice-to-slice algorithm. Systematic parameter optimization may result in more successful registrations, leading to more accurate geometric models.

5. ACKNOWLEDGEMENTS

This work was supported by the Canadian Institutes of Health Research and by the Natural Sciences and Engineering Research Council of Canada.

6. REFERENCES

[1] Chakravarty, M.M., Bertrand, G., Hodge, C.P., Sadikot, A.F., Collins, D.L. (2006). The creation of a brain atlas for image guided neurosurgery using serial histological data. *NeuroImage*, 30, 359–376.

[2] Collins, D.L., Evans, A.C. (1997). ANIMAL: validation and application of non-linear registration based segmentation. *Int. J. Pattern Recogn. Artif. Intell.*, 11, 1271–1294.

[3] Funnell, W.R.J., Khanna, S.M., Decraemer, W.F. (1992). On the degree of rigidity of the manubrium in a finite-element model of the cat eardrum. *J. Acoust. Soc. Am.*, 91, 2082-2090.

[4] Nambiar, S., Chakravarty, M.M., Funnell, W.R.J., Collins, D.L. (2007). Non-linear registration of histological images for 3-D middle-ear modelling. *Can. Acoustics*, 35, 78-79.

[5] Sun, Q., Gan, R.Z., Chang, K.H., Dormer, K.J. (2002) Computer-integrated finite element modeling of human middle ear. *Biomechan. Model. Mechanobiol.*, 1, 109-122.

[6] Warrick, P.A., Funnell, W.R.J. (1998): A VRML-based anatomical visualization tool for medical education. *IEEE Trans. Inf. Technol. Biomed.,* 2, 55-61